

# Different Effect of Media Opacity on Vessel Density Measured by Different Optical Coherence Tomography Angiography Algorithms

Jinyu Zhang<sup>1</sup>, Fang Yao Tang<sup>2</sup>, Carol Y. Cheung<sup>2</sup>, and Haoyu Chen<sup>1</sup>

<sup>1</sup> Joint Shantou International Eye Center, Shantou University and the Chinese University of Hong Kong, Shantou, China

<sup>2</sup> Department of Ophthalmology and Visual Sciences, the Chinese University of Hong Kong, Hong Kong, China

**Correspondence:** Haoyu Chen, Joint Shantou International Eye Center Shantou University and the Chinese University of Hong Kong, North Dongxia Road, Shantou, 515041, China. e-mail: [drchenhaoyu@gmail.com](mailto:drchenhaoyu@gmail.com)

**Received:** November 6, 2019

**Accepted:** April 2, 2020

**Published:** July 13, 2020

**Keywords:** media opacity; optical coherence tomography angiography; algorithm

**Citation:** Zhang J, Tang FY, Cheung CY, Chen H. Different effect of media opacity on vessel density measured by different optical coherence tomography angiography algorithms. *Trans Vis Sci Tech.* 2020;9(8):19. <https://doi.org/10.1167/tvst.9.8.19>

**Purpose:** Several studies show that media opacity reduces vessel density (VD) measured by image processing algorithms of optical coherence tomography angiography (OCTA). However, different models of OCTA designed their own algorithms and computational methods, which may have different effects of opacity on VD. This study is aimed to investigate the impact of a simulated model of media opacity on quantitative measurement of two OCTA devices.

**Methods:** A spectral-domain based OCTA (Cirrus 5000; Carl Zeiss Meditec) and a swept-source based OCTA (Triton DRI-OCT, Topcon Inc.) were used to image retinal microvasculature at the macula using  $3 \times 3$  mm scanning protocol from 22 eyes of 22 healthy subjects. Media opacity was simulated with neutral-density filters (optical density (OD) <sub>$\lambda=840\text{nm}$</sub>  ranges 0.10–0.48 in Cirrus; OD <sub>$\lambda=1050\text{nm}$</sub>  ranges 0.15–0.51 in Triton). The filters were placed in front of each study eye, and signal strength (SS) or signal strength intensity (SSI) was recorded during imaging. The parafoveal VD of superficial capillary plexus was then measured using the built-in software from the two devices. The correlations among OD, SS/SSI, and VD were analyzed.

**Results:** Increased OD was significantly correlated with decreased SS and SSI ( $r_s = -0.576$  and  $-0.922$ , respectively, both  $P < 0.001$ ) in Cirrus and Triton, respectively. Although increased OD was significantly correlated with decreased VD in Cirrus ( $r_s = -0.539$ ,  $P < 0.001$ ), there was no significant correlation between OD with VD in Triton ( $r_s = -0.143$ ,  $P = 0.137$ ).

**Conclusions:** The effect of media opacity on quantitative measurement of VD is different between different Cirrus and Triton OCTA devices.

**Translational Relevance:** This study demonstrates that the effect of media opacity on VD measurement is different among different OCTA devices, suggesting that caution must be taken when interpreting VD measurement on OCTA, particularly among individuals with media opacity.

## 摘要:

**目的:** 屈光介质混浊会降低光相干断层扫描血管成像(optical coherence tomography angiography, OCTA) 定量测量视网膜血管密度的结果。不同类型的OCTA运用的算法不同,得出的测量结果可能不同。本课题的目的是研究屈光介质混浊对Cirrus 5000 OCTA及DRI Triton OCTA定量测量结果的影响。

**方法:** 对22名屈光介质透明的健康成年人用Cirrus 5000 和 DRI Triton OCTA, 分别在无滤光片(光密度为0)及滤光片(光密度为0.10–0.48, Cirrus; 光密度0.15–0.51, DRI Triton)模拟屈光介质混浊的条件下用 $3 \times 3$ mm血流成像模式扫描右眼黄斑区视网膜。使用OCTA自带测量软件记录和测量图像信号分数、旁中心凹浅层血管密度等数据。比较不同透光率下各参数的变化。

**结果:** 随着光密度的增加, Cirrus 5000 OCTA旁中心血管密度及图像信号分数减少 ( $r_s = -0.539$ ,  $p < 0.001$  and  $r_s = -0.576$ ,  $p < 0.001$ );旁中心血管密度随信号分数的增加而

增加 ( $r_s = 0.471, p < 0.001$ )。随着光密度的增加, DRI Triton OCTA图像信号分数减少 ( $r_s = -0.922, p < 0.001$ ), 但旁中心血管密度与光密度或信号分数不相关 ( $r_s = -0.143, p = 0.137$  and  $r_s = -0.009, p = 0.924$ )。

**结论:** 屈光介质混浊对Cirrus 5000 和 DRI Triton OCTA定量测量结果的影响不同。

## Introduction

High-resolution retinal microvasculature can now be imaged noninvasively, safely, and rapidly with optical coherence tomography angiography (OCTA).<sup>1,2</sup> Furthermore, quantitative OCTA assessment, such as vessel density (VD) and foveal avascular zone (FAZ) area, can be measured reliably and are being proposed to be a biomarker for macular ischemia in diabetic retinopathy and other retinal vascular diseases.<sup>3,4</sup>

Media opacity, such as cataract, often presented in the eyes of elderly, can reduce the light entering into the eyes and, therefore, influence the backscattering of light detected by the OCTA devices. For example, studies have shown that media opacity, worsening image quality of OCT, and influences of quantitative measurement of retinal nerve fiber layer thickness,<sup>5-8</sup> as well as diagnosis of glaucoma or glaucoma progression.<sup>9</sup> OCTA imaging is derived from the OCT signal. Therefore, quantitative measurement on OCTA is expected to be affected by media opacities as a matter of course. A few studies have previously reported that VD measurement is reduced in the presence of media opacity in OCTA devices.<sup>10,11</sup>

Different OCTA devices have different wavelengths of light source, image processing algorithms, and computational methods.<sup>12</sup> Therefore, the effect of media opacity on quantitative OCTA measurement is presumably variable in different OCTA devices.

In the present study, we used natural-density (ND) filters to simulate different degrees of media opacity optically, and compared the impact of media opacity on VD measurement between two different OCTA devices.

## Materials and Methods

### Subjects

In this cross-sectional study, healthy Chinese subjects between 21 and 28 years of age were recruited. Only the right eye from each subject was included. All measurements were obtained in a very similar environment using the same OCTA devices, which

were operated by a trained technician. All participants had normal retinas and did not have any media opacities. All the study eyes had best-corrected visual acuity of at least 20/25 using the Snellen chart, intraocular pressure  $< 21$  mm Hg, and refractive error within  $\pm 6$  diopter(D). Subjects were excluded if they had any evidence of systemic or ocular diseases. The research followed the tenets of the Declaration of Helsinki and was approved by the Ethics Review Board of Joint Shantou International Eye Center of Shantou University and the Chinese University of Hong Kong.

The hypotheses are that the mean of each time is equal ( $H_0$ ) and at least two of the means of each time is unequal ( $H_1$ ). The sample size was calculated according to multiple sample 1-way analysis of variance model<sup>13</sup>:

$$n = \psi^2 \left[ \sum_{i=1}^k S_i^2/k \right] / \left[ \sum_{i=1}^k (\bar{X}_i - \bar{X})^2/(k-1) \right],$$

where  $S_i$  is the SD of VD each time,  $\bar{X}_i$  is the mean of each time, and  $\bar{X}$  is the mean of  $k$  time means. These parameters were calculated from preliminary examination of five eyes. The  $k$  is the time counts, which is 6 for Cirrus and 5 for Triton,  $\alpha$  is the rate of type 1 error, and  $\beta$  is the rate of type 2 error, and they were set as  $\alpha = 0.05$  and  $\beta = 10\%$ . The  $\psi$  is found from  $\psi$  table according to the degree of freedom  $k-1$ . The sample size was estimated as 14 for Cirrus and 18 for Triton. In this study, we included 22 subjects.

### Light Attenuation Model

There are three types of optical disturbances: light attenuation, refractive aberrations, and light scattering/straylight.<sup>7</sup> Previous studies showed that light attenuation in the optical coherence tomography (OCT) and OCTA scanning spot on the retina, expressed as optical density (OD), fully determined loss of OCT and OCTA image quality as provided by the OCT and OCTA systems, irrespective of the nature of the filter, or type of cataract.<sup>7,11,14</sup> ND filters have been used to simulate the light attenuation character of media opacity in previous studies.<sup>6,10</sup> In the current study, two sets of ND filters (ZAB, PHTODE, CHINA) with known OD were used to simulate media opacity optically for Cirrus OCTA (5 ND filters ranged from 0.10 to 0.48 with wavelength of 840 nm), and

**Table 1.** Single Pass Optical Density Values (in Log Units) of the ND Filters

Filter Nominal Value T <sub>visible light</sub> (%)	Cirrus OCTA		Triton OCTA	
	T <sub>λ=840nm</sub> (%)	OD <sub>λ=840nm</sub> (single pass)	T <sub>λ=1050nm</sub> (%)	OD <sub>λ=1050nm</sub> (single pass)
80	80	0.10	70	0.15
70	60	0.22	50	0.30
60	53	0.28	43	0.37
50	42	0.38	31	0.51
35	33	0.48	–	–

ND, neutral density; T, transmittance; OD, optical density.

Triton OCTA (4 ND filters ranged from 0.15 to 0.51 with wavelength of 1050 nm), respectively.

The ND filters have different transmittance (T) at different wavelengths, and T has a logarithmic relationship with OD:  $OD = \lg(1/T)$ . When the OD is similar, the effect of wavelength is similar. We used OD to represent each filter value as the following:  $OD_{\lambda=840nm} = 0.10, 0.22, 0.28, 0.38, \text{ and } 0.48$  on Cirrus OCTA; and  $OD_{\lambda=1050nm} = 0.15, 0.30, 0.37, \text{ and } 0.51$  on Triton OCTA (Table 1). This resulted in six scans of Cirrus OCTA and five scans of Triton OCTA from the same region in each eye. Although the ODs were different between the two devices, we did not directly compare the VD between the two devices, but analyzed the correlation of OD and VD in each device.

## OCTA Imaging Protocol

The pupils of all subjects were dilated to at least 6 mm diameter with topical 0.5% tropicamide. Two OCTA devices were used: a spectral-domain OCT device (Cirrus HD-OCT 5000; Carl Zeiss, Dublin, CA) and a swept-source OCT device (DRI-OCT Triton; Topcon, Inc., Tokyo, Japan). The central wavelength of Cirrus is 840 nm and it uses an intensity and phase differentiation-based algorithm for OCTA imaging (OCT microangiography-complex [OMAG]).<sup>15</sup> The central wavelength of Triton is 1050 nm and it uses an amplitude decorrelation ratio-based algorithm for OCTA imaging (OCT angiography ratio analysis [OCTARA]).<sup>16</sup> The macular 3 × 3 mm scanning protocol was used for OCTA imaging (Cirrus: 245 B-scans in total, 245 A-scans in each B-scan, and each B-scan is repeated 4 times<sup>15</sup>; Triton: 320 B-scans in total, 320 A-scans in each B-scan, and each B-scan is repeated 4 times).<sup>17</sup>

During OCTA imaging, each ND filter was positioned in front of the eye by using a fixed frame. We carefully checked the positioning of the filters (e.g. potential tilt of the filters) before OCTA imaging. The

tilt of filter was estimated to be < 10°. In this manner, a maximum error of 2% was accepted.<sup>5</sup> OCTA imaging was first performed without filter (native) and subsequently with ND filters.

All study subjects were first tested with the Cirrus OCTA, and then with the Triton OCTA. All the subjects were instructed to close their eyes before and after each OCTA scan to avoid the effect of corneal dryness and fatigue. Artificial tears were given if any subjects eyes felt dry or fatigued. Quality control was performed during OCTA scanning. We excluded any OCTA image with poor quality due to significant image artifacts and poor centration, including blink, and doubling of the retinal vessels. Presence of > 5 artifacts were considered as severe artifacts,<sup>12</sup> and decentration artifact was considered moderate to severe if the central or inner subfields were < 10% outside the OCT grid after manual reposition.<sup>18</sup> Images with severe motion or decentration artifacts > 10% outside the OCT grid were also excluded. Repeated scanning was performed if the OCTA image deemed poor image quality.

## Quantitative Measurements

The OCTA images were analyzed using its own built-in software. For Cirrus, AngioPlex software (version 10.0) was used. Signal strength (SS; ranged from 0–10) and parafoveal VD of superficial capillary plexus (SCP) were automatically measured, and there was no error of retinal layer segmentation. For Triton, ImageNet software (version 6.0) was used. The signal strength intensity (SSI; ranged from 0–100) and parafoveal VD of SCP were automatically generated after the error of retina layer segmentation was corrected manually.

Parafoveal VD is divided into subfields (include inner superior, inner nasal, inner inferior, and inner temporal) according to the Early Treatment of Diabetic Retinopathy Study (ETDRS). It is noted that the inner

**Table 2.** Baseline Characteristics

Characteristics	Mean $\pm$ SD	Range
Age (y)	25 $\pm$ 2	21–28
Male / Female	3/19	–
IOP (mm Hg)	15 $\pm$ 2	12–18
BCVA (log MAR)	–0.07 $\pm$ 0.07	–0.18 to 0.05
SE (D)	–2.02 $\pm$ 2.14	–5.25 to 3.75

IOP, intraocular pressure; BCVA, best-corrected visual acuity;

SE, spherical equivalent; D, diopter.

diameter of parafovea is 1 mm for both devices, and the outer diameter is 3.0 mm in Cirrus, but 2.5 mm in Triton.

## Statistical Analysis

VD at different regions without filters was taken as baseline measurement. We used percent VD in the analysis, which was calculated as VD divided by its baseline value.

SS, SSI, and percent VD were reported as mean  $\pm$  SD. Correlation of OD with change in percent VD and SS / SSI by the effect of ND filter was performed using Spearman correlation test. Change in percent parafoveal VD as the result of OD change was evaluated with repeated measurements ANOVA test, adjusted for multiple testing with a Least Significant Difference (LSD) test as the post hoc analysis. Statistics were calculated by SPSS (IBM, SPSS statistics, version 19; SPSS Inc., Chicago, IL), and statistical significance was defined as  $P < 0.05$ . Bland-Altman plots were used to demonstrate the agreement of VD between without filter and with different filters (5 in Cirrus and 4 in Triton) of VD graphically.

## Results

Twenty-two right eyes of 22 healthy volunteers were included in this study. Table 2 shows the characteristics of the study participants. The mean  $\pm$  SD of refractive error was  $-2.02 \pm 2.14$  D (range:  $-5.25$ – $3.75$  D) in the right eye.

Figure 1A shows a series of structural B-scans of the two OCTA devices. The boundaries of retinal layers became more indistinct as OD increased in both devices. Figure 1B shows correlations between OD with SS of Cirrus ( $r_s = -0.576$ ,  $P < 0.001$ ) and SSI of Triton ( $r_s = -0.922$ ,  $P < 0.001$ ). Table 3 shows the differences found in SS / SSI between scans obtained from different ND filters.

Figure 2A shows a series of OCTA images with different ND filters. We found that percent parafoveal VD decreased as  $OD_{\lambda=840\text{nm}}$  increased in Cirrus ( $r_s = -0.539$ ,  $p < 0.001$ ), whereas no correlation was found between parafoveal VD and  $OD_{\lambda=1050\text{nm}}$  in Triton ( $r_s = -0.143$ ,  $P = 0.137$ ). In the post hoc analysis, percent parafoveal VD of Cirrus appeared to decrease beyond a threshold  $OD_{\lambda=840\text{nm}}$  of 0.22. When the  $OD_{\lambda=840\text{nm}}$  was 0.38, percent parafoveal VD was decreased to  $11.7 \pm 2.5\%$  ( $P < 0.001$ ). Percent parafoveal VD of Triton changed variously in the post hoc analyses. When  $OD_{\lambda=1050\text{nm}}$  were 0.15, 0.30, and 0.37, percent parafoveal VD was decreased to  $0.9 \pm 0.6\%$  ( $P = 0.151$ ),  $1.7 \pm 0.5\%$  ( $P = 0.003$ ), and  $1.8 \pm 0.5\%$  ( $P = 0.002$ ), respectively. However, parafoveal VD was increased to  $0.5 \pm 0.4\%$  ( $P = 0.309$ ) when  $OD_{\lambda=1050\text{nm}}$  was 0.51 (see Table 3).

Figure 2B shows the correlations between OD and different regions of parafoveal VD. We found that OD was significantly correlated with VD of subregions (inner superior, inner nasal, inner inferior, and inner temporal) in both Cirrus ( $r_s = -0.476$ ,  $-0.438$ ,  $-0.431$ , and  $-0.478$ ,  $P < 0.001$ , respectively) and Triton ( $r_s = 0.047$ ,  $-0.093$ ,  $-0.100$ , and  $-0.072$ ,  $P = 0.627$ ,  $0.332$ ,  $0.297$ , and  $0.454$ , respectively).

Bland-Altman plots also showed that as the OD increased, the bias of VD between no filter and with filter increased on Cirrus (Supplementary Fig. S1). However, the bias VD between no filter and with filter did not correlate with OD in Triton (Supplementary Fig. S2).

Although percent parafoveal VD of Cirrus was correlated with SS ( $r_s = 0.471$ ,  $P < 0.001$ ; Fig. 3A), there was no correlation between percent parafoveal VD and SSI in Triton ( $r_s = -0.009$ ,  $P = 0.924$ ; Fig. 3B).

## Discussion

In this study, we found a correlation between an increase in  $OD_{\lambda=840\text{nm}}$ , and a decrease in percent VD of Cirrus, whereas there was no correlation between  $OD_{\lambda=1050\text{nm}}$  and percent VD of Triton. We also found that percent VD decreased as SS decreased in Cirrus OCTA, but percent VD was unchanged as SSI decreased in Triton OCTA. Our study suggested that the impact of media opacity on VD measurement is different between these two OCTA devices.

Previous studies have shown a significant increase of macular VD after cataract surgery tested by Zeiss PLEX Elite 9000 with OMAG algorithm and Optovue RTVue-XR Avanti with SSADA algorithm.<sup>19,20</sup> Although these studies suggested that

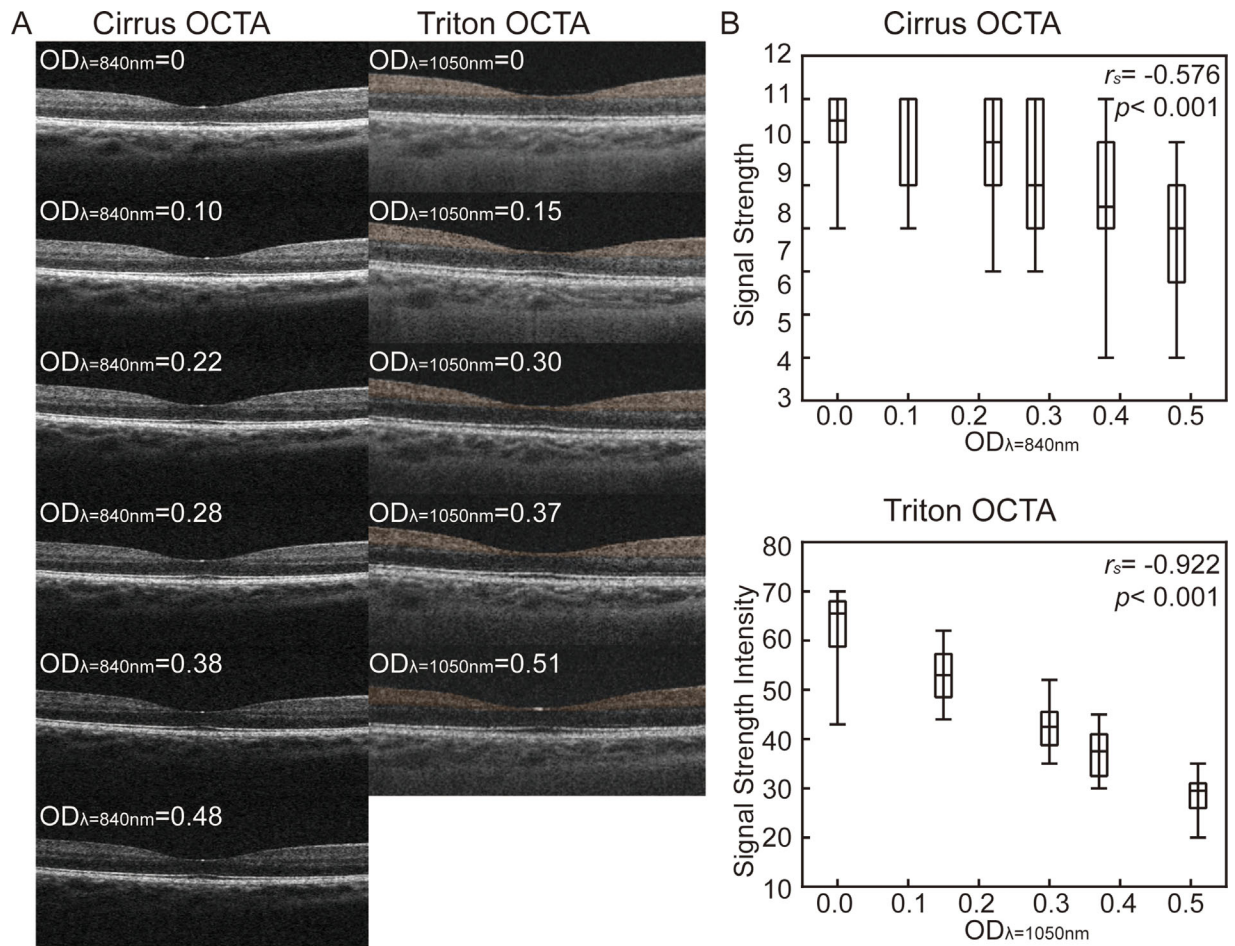


**Figure 1.** B-scan and signal strength (signal strength intensity) illustrating the effect of neutral density filters on macular OCTA image acquisition. **(A)** B-scan of OCTA in different OD. **(B)** Box plot of the difference and correlation between OD and signal strength (signal strength intensity). Upper and lower whiskers show the maximum and minimum difference. The  $r_s$  and  $P$  value are shown ( $n = 22$ ). OD, optical density;  $r_s$ , Spearman correlation coefficient.

**Table 3.** Signal Score and Percent Parafoveal Vessel Density Change per Filter of OCTA

Cirrus OCTA		Triton OCTA							
OD <sub>λ=840nm</sub>	SSMean ± SD	Parafoveal VD (%)	P Value*	Δparafoveal VD 95% CI (%)	OD <sub>λ=1050nm</sub>	SSIMean ± SD	Parafoveal VD (%)	P Value*	Δparafoveal VD 95% CI (%)
0.00	9.32 ± 0.84	100.00	–	–	0.00	63.6 ± 6.8	100.00	–	–
0.10	9.23 ± 1.07	98.8 ± 12.3	0.644	1.2 (–4.2 to 6.7)	0.15	53.2 ± 5.4	99.1 ± 2.8	0.151	0.9 (–0.3 to 2.1)
0.22	8.55 ± 1.37	93.8 ± 12.1	0.026	6.2 (0.8 – 11.5)	0.30	42.9 ± 5.1	98.3 ± 2.4	0.003	1.7 (0.7 – 2.8)
0.28	8.23 ± 1.52	92.0 ± 10.8	0.002	8.0 (3.2 – 12.8)	0.37	36.2 ± 4.4	98.2 ± 2.5	0.002	1.8 (0.7 – 2.9)
0.38	7.68 ± 1.52	88.3 ± 11.9	< 0.001	11.7 (6.4 – 16.9)	0.51	28.0 ± 4.2	99.5 ± 2.1	0.309	0.5 (–0.5 to 1.4)
0.48	6.59 ± 1.53	78.2 ± 17.1	< 0.001	21.8 (14.2 – 29.4)	–	–	–	–	–

OD, optical density; SS, signal strength; SSI, signal strength intensity; SD, standard deviation; VD, vessel density; CI, confidence interval.

\*LSD,  $P$  value of repeated-measurements ANOVA.  $P$  is significant at 0.05.

elimination of media opacity resulted in increase of VD measurement, it did not exclude the factor of retinal vasculature change due to cataract surgery. It has been reported that ND filters as a beam attenuation

can decrease the flow signal and VD by using Optovue RTVue-XR Avanti,<sup>11</sup> both SS index and VD decreased linearly with OD of the ND filter, and VD decreased as SS index decreased by using two different OCTA

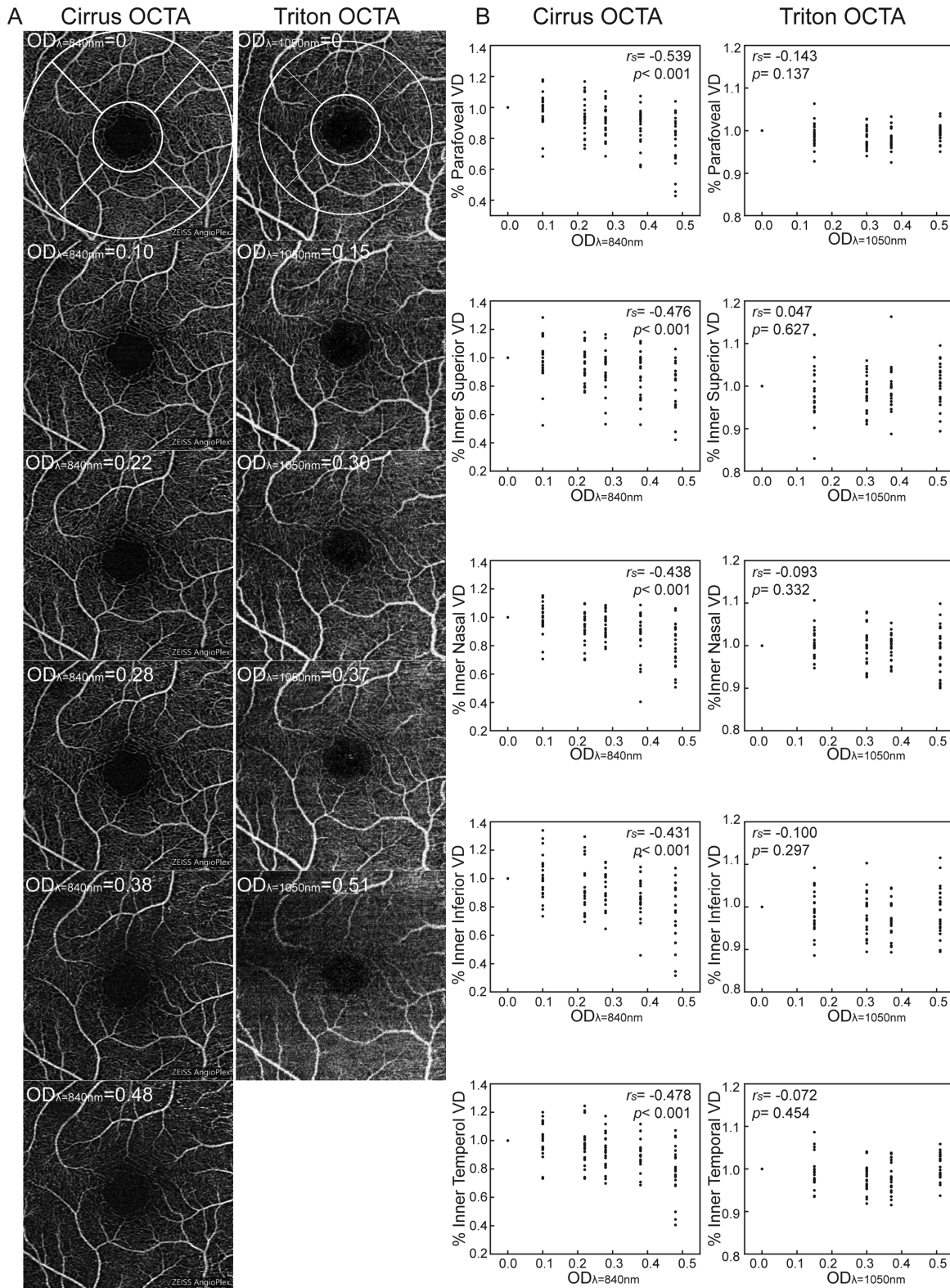


**Figure 2.** SCP and VD illustrating the effect of ND filters on macular OCTA image acquisition. **(A)** SCP in different OD. The VD of SCP is divided by an ETDRS grid includes parafovea (the annulus area between the two white circles) that contains four regions (inner superior, nasal, inferior, and temporal). The diameter of small white and big white circles is 1.0 mm and 3.0 mm in Cirrus OCTA (2.5 mm in Triton OCTA), respectively. **(B)** Scatter plots and correlation between OD and each region of parafoveal VD in SCP. Each point from one participant. The  $r_s$  and  $P$  values were shown ( $n = 22$ ). SCP, superficial capillaries plexus; VD, vessel density; OD, optical density; ETDRS, early treatment diabetic retinopathy study;  $r_s$ , Spearman correlation coefficient.

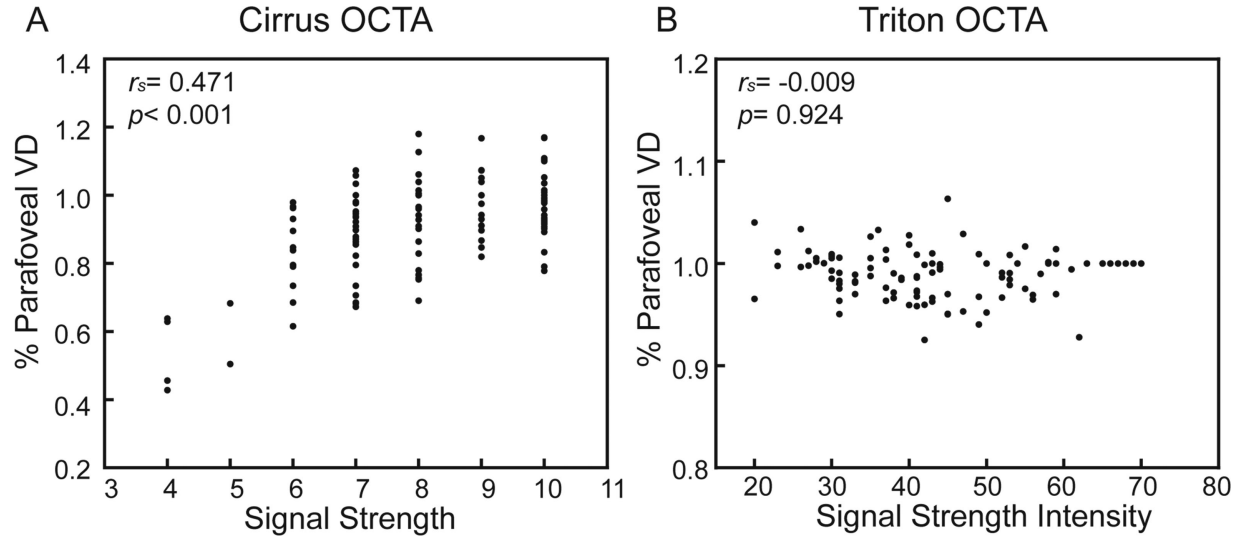


**Figure 3.** Scatter plots between signal strength (signal strength intensity) and parafoveal VD of OCTA image. **(A)** Scatter plots and correlation between signal strength and parafoveal VD of Cirrus OCTA image. **(B)** Scatter plots and correlation between signal strength intensity and parafoveal VD of Triton OCTA image. Each point from one scan. The  $r_s$  and  $P$  values were shown ( $n = 22$ ). VD, vessel density;  $r_s$ , Spearman correlation coefficient.

devices (Cirrus and Optovue RTVue-XR Avanti).<sup>10</sup> In our study, the results with Cirrus are similar to previous studies using Cirrus and Optovue RTVue-XR Avanti. However, we found that the effect of media opacity on VD measurement was different in Triton. Specifically, we found that the values of percent VD were similar to  $OD_{\lambda=1050\text{nm}}$  increased or SSI decreased in Triton.

Several possibilities may explain the different effect of media opacity on VD measurement between the two devices. First, it may due to the calculation in the OCTA image processing algorithms. The different algorithms of OCTA signal flow between two devices may contribute to different effect of media opacity on VD measurement. The OMAG algorithm in Cirrus is based on the following formula:

$$Flow(x, z) = \frac{1}{R-1} \sum_{i=0}^{R-1} [C_{i+1}(x, z) - C_i(x, z)], \quad (1)$$

where  $i$  is the index for the repeated time of B-scans at each  $y$ -scan position,  $x$  is the fast axis scan position,  $z$  is the depth,  $R$  is the number of repeated B-scans in each step, and  $C$  is the motion-corrected complex OCT signal, which incorporates both intensity and phase information from repeated B-scans at the same position.<sup>15</sup> Intensity is an important component of complex. In media opacity, increased  $OD_{\lambda=840\text{nm}}$  caused decreased SS, decreased intensity, and decreased  $C$ . A new parameter “ $a$ ” is introduced in the formula to represent the change of OCT signal,  $C' = aC$ ,  $a < 1$  to represent the reduction of OCT

signal, and the flow signal in media opacity is:

$$\begin{aligned} Flow(x, z)' &= \frac{1}{R-1} \sum_{i=0}^{R-1} [C'_{i+1}(x, z) - C'_i(x, z)] \\ &= \frac{1}{R-1} \sum_{i=0}^{R-1} [aC_{i+1}(x, z) - aC_i(x, z)] \quad (2) \\ &= a \frac{1}{R-1} \sum_{i=0}^{R-1} [C_{i+1}(x, z) - C_i(x, z)] \\ &= aFlow(x, z) \end{aligned}$$

As  $a < 1$ , then  $Flow(x, z)' < Flow(x, z)$  in Cirrus OCTA. The Triton OCTA OCTARA algorithm is based on decorrelation ratio  $r$ , between corresponding image pixels as follows:

$$r(x, y) = 1 - \frac{1}{N} \sum_{i,j} \frac{\min[I_i(x, y), I_j(x, y)]}{\max[I_i(x, y), I_j(x, y)]}, \quad (3)$$

where  $I(x, y)$  is the OCT signal intensity,  $N$  is the number of scanned B-scan combinations at a given location, and  $i$  and  $j$  represent two frames within any given combination of frames.<sup>16</sup> In media opacity,  $OD_{\lambda=1050\text{nm}}$  increased, caused SSI to decrease, and  $I$  to decrease ( $I' = aI$ ,  $a < 1$ ).

$$\begin{aligned} r(x, y)' &= 1 - \frac{1}{N} \sum_{i,j} \frac{\min[I'_i(x, y), I'_j(x, y)]}{\max[I'_i(x, y), I'_j(x, y)]} \\ &= 1 - \frac{1}{N} \sum_{i,j} \frac{a \times \min[I_i(x, y), I_j(x, y)]}{a \times \max[I_i(x, y), I_j(x, y)]} \quad (4) \\ &= 1 - \frac{1}{N} \sum_{i,j} \frac{\min[I_i(x, y), I_j(x, y)]}{\max[I_i(x, y), I_j(x, y)]} = r(x, y) \end{aligned}$$

Therefore, the flow signal remains unchanged in Triton OCTA in the presence of media opacity. In brief, the algorithms of OCTA flow signal are different between these two devices. The algorithm of Cirrus OCTA is based on the difference of sequential scans. As OD increases, OCT signal decreases proportionally, OCTA flow signal, which is the difference of two sequential OCT scan decreases, so the vessel density decreases, although the algorithm of Triton OCTA is based on the ratio of sequential scan. As OD increases, OCT signal decreases proportionally, but OCTA flow signal, which is the ratio of the two sequential OCT scan remains unchanged, therefore, the vessel density does not change.

It should be noted that the light source of the two OCTA devices may also affect the VD measurement. A swept-source OCT device has better penetration compared to a spectral-domain OCT device in patients with media opacity.<sup>21</sup> In addition, the range of OD differs between the two OCTA devices and the relationship between OD and VD may be nonlinear. Therefore, different wavelengths may explain partially different VD results in the two devices.

VD quantification using OCTA has a wide range of diagnostic and prognostic application in glaucoma and retinal diseases.<sup>22–25</sup> Cataract or other media opacity, such as corneal scar and vitreous hemorrhage, are common in clinics. Caution must be taken when interpreting VD measurement on OCTA in individuals with media opacity, in which VD may be reduced or unchanged, depending on the OCTA device used.

Although our hypothesis was supported statistically, some limitations are worth noting. First, the VD measured from the two OCTA devices were measured in different areas (the diameter of parafoveal area in Cirrus was 3 mm, whereas Triton was 2.5 mm), which may cause a difference in the VD measurement. Second, we only reported the VD of the SCP at the macula. The reason for not assessing the deep vessel parameters is that it is difficult to eliminate projection artifacts of vessels from the superficial vascular network in the deep vascular network. Third, some of the SCPs exhibit mild motion and (or) decentration artifacts, which may have affected the VD measurement as well as the correlation of OD. Fourth, the present study only demonstrated the difference of these two devices, but has not developed any algorithms to correct the impact of media opacity on VD measurement, which will be the subject of future studies. Fifth, the current study only used ND filters for mimic light attenuation. Other types of optical disturbances (refractive aberrations and light scattering) were not used.<sup>7</sup> Finally, the performance of algorithms may be different between ischemic retina and normal retina.

The accuracy in healthy subjects is the first step and we intend to investigate the effect of media opacity on VD measurement in diseased eyes in further studies.

In conclusion, the effect of media opacity on quantitative VD measurement is different for Cirrus OCTA and Triton OCTA possibly due to different OCTA flow algorithms used by different models.

## Acknowledgments

Supported by the grant for Key Disciplinary Project of Clinical Medicine under the Guangdong High-level University Development Program (002-18119101) and the Intramural grant of Joint Shantou International Eye Center (19-004).

Disclosure: **J. Zhang**, None; **F.Y. Tang**, None; **C.Y. Cheung**, None; **H. Chen**, None

## References

1. Spaide RF, Fujimoto JG, Waheed NK, Sadda SR, Staurengi G. Optical coherence tomography angiography. *Prog Retin Eye Res.* 2018;64:1–55.
2. Spaide RF, Jr KJM, Cooney MJ. Retinal vascular layers imaged by fluorescein angiography and optical coherence tomography angiography. *JAMA Ophthalmol.* 2015;133:45–50.
3. Kim AY, Chu Z, Shahidzadeh A, Wang RK, Puliafito CA, Kashani AH. Quantifying microvascular density and morphology in diabetic retinopathy using spectral-domain optical coherence tomography angiography. *Invest Ophthalmol Vis Sci.* 2016;57:OCT362–OCT370.
4. Falavarjani KG, Shenazandi H, Naseri D, et al. Foveal avascular zone and vessel density in healthy subjects: an optical coherence tomography angiography study. *J Ophthalmic Vis Res.* 2018;13:260–265.
5. Darma S, Kok PH, van den Berg TJ, et al. Optical density filters modeling media opacities cause decreased SD-OCT retinal layer thickness measurements with inter- and intra-individual variation. *Acta Ophthalmol.* 2015;93:355–361.
6. Tappeiner C, Barthelmes D, Abegg MH, Wolf S, Fleischhauer JC. Impact of optic media opacities and image compression on quantitative analysis of optical coherence tomography. *Invest Ophthalmol Vis Sci.* 2008;49:1609–1614.
7. Kok PH, van Dijk HW, van den Berg TJ, Verbraak FD. A model for the effect of disturbances in



- the optical media on the OCT image quality. *Invest Ophthalmol Vis Sci.* 2009;50:787–792.
8. Lee DW, Kim JM, Park KH, Choi CY, Cho JG. Effect of media opacity on retinal nerve fiber layer thickness measurements by optical coherence tomography. *J Ophthalmic Vis Res.* 2010;5:151–157.
  9. Sanchez-Cano A, Pablo LE, Larrosa JM, Polo V. The effect of phacoemulsification cataract surgery on polarimetry and tomography measurements for glaucoma diagnosis. *J Glaucoma.* 2010;19:468–474.
  10. Yu JJ, Camino A, Liu L, et al. Signal strength reduction effects in OCT angiography. *Ophthalmol Retina.* 2019;3:835–842.
  11. Gao SS, Jia Y, Liu L, et al. Compensation for reflectance variation in vessel density quantification by optical coherence tomography angiography. *Invest Ophthalmol Vis Sci.* 2016;57:4485–4492.
  12. Munk MR, Giannakaki-Zimmermann H, Berger L, et al. OCT-angiography: a qualitative and quantitative comparison of 4 OCT-A devices. *PLoS One.* 2017;12:e0177059.
  13. Yan H, Xu Y, Zhao N. Medical Statistics, 2nd ed. *Beijing, People's Medical Publishing House.* 2010;268:513.
  14. Kok PH, van den Berg TJ, van Dijk HW, et al. The relationship between the optical density of cataract and its influence on retinal nerve fibre layer thickness measured with spectral domain optical coherence tomography. *Acta Ophthalmol.* 2013;91:418–424.
  15. Rosenfeld P, Durbin M, Miller A, et al. ZEISS Angioplex™ spectral domain optical coherence tomography angiography: technical aspects. *Dev Ophthalmol.* 2016;56:18–29.
  16. Stanga P, Tsamis E, Papayannis A, Stringa F, Cole T, Jalil A. Swept-Source Optical Coherence Tomography Angio™ (Topcon Corp, Japan): technology review. *Dev Ophthalmol.* 2016;56:13–17.
  17. Ohayon A, Sacconi R, Semoun O, Corbelli E, Souied EH, Querques G. Choroidal neovascular area and vessel density comparison between two swept-source optical coherence tomography angiography devices. *Retina.* 2020;40:521–528.
  18. Holmen IC, Konda MS, Pak JW, et al. Prevalence and severity of artifacts in optical coherence tomographic angiograms. *JAMA Ophthalmol.* 2019;138:119–126.
  19. Yu S, Frueh B, Steinmair D, et al. Cataract significantly influences quantitative measurements on swept-source optical coherence tomography angiography imaging. *PLoS One.* 2018;13:e0204501.
  20. Zhao Z, Wen W, Jiang C, Lu Y. Changes in macular vasculature after uncomplicated phacoemulsification surgery: optical coherence tomography angiography study. *J Cataract Refract Surg.* 2018;44:453–458.
  21. Novais EA, Adhi M, Moulton EM, et al. Choroidal neovascularization analyzed on ultrahigh-speed swept-source optical coherence tomography angiography compared to spectral-domain optical coherence tomography angiography. *Am J Ophthalmol.* 2016;164:80–88.
  22. Liang MC, Witkin AJ. Optical coherence tomography angiography of mixed neovascularizations in age-related macular degeneration. *Dev Ophthalmol.* 2016;56:62–70.
  23. Zhang M, Hwang TS, Dongye C, Wilson DJ, Huang D, Jia Y. Automated quantification of nonperfusion in three retinal plexuses using projection-resolved optical coherence tomography angiography in diabetic retinopathy. *Invest Ophthalmol Vis Sci.* 2016;57:5101–5106.
  24. Kashani AH, Chen CL, Gahm JK, et al. Optical coherence tomography angiography: a comprehensive review of current methods and clinical applications. *Prog Retin Eye Res.* 2017;60:66–100.
  25. Takusagawa HL, Liu L, Ma KN, et al. Projection-resolved optical coherence tomography angiography of macular retinal circulation in glaucoma. *Ophthalmology.* 2017;124:1589–1599.